Mechanically activated molecular switch through single-molecule pulling: Supplementary Information

Ignacio Franco, Christopher B. George, Gemma C. Solomon, George C. Schatz, and Mark A. Ratner

Department of Chemistry, Northwestern University, Evanston, Illinois 60208-3113

(Dated: December 14, 2010)

Pulling simulation force field parameters: Additional MM3 force field parameters required to describe the stacker were obtained through standard quantum chemistry computations using HF/6-31G(d,p). Using the notation of Ref. 30 of the paper, the additional required parameters are: (i) C(sp2)-S bond stretching, $l_0 = 1.776$ Å, $k_s = 3.8$ mdyne/Å^2, where l_0 is the equilibrium bond length and k_s the stretching parameter; (ii) Angle bending: C(sp2)-C(sp2)-S, $\theta_0 = 122.8^o$, $k_\theta = 1.5$ mdyne Å/rad^2; H-C(sp2)-S, $\theta_0 = 115.4^o$, $k_\theta = 1.4$ mdyne Å/rad^2; C(sp2)-S-H, $\theta_0 = 97.3^o$, $k_\theta = 1.1$ mdyne Å/rad^2, where θ_0 is the equilibrium angle and k_θ the angle-bending constant; (iii) Torsional coefficients for C(sp2)-C(sp2)-S-H: $V_1 = 1.5568$, $V_2 = 0.2992$ and $V_3 = -1.2977$ kcal/mol, where the torsional energy for dihedral angle ω is given by $E_\omega = (V_1/2)(1+\cos\omega)+(V_2/2)(1-\cos 2\omega)+(V_3/2)(1+\cos 3\omega)$.

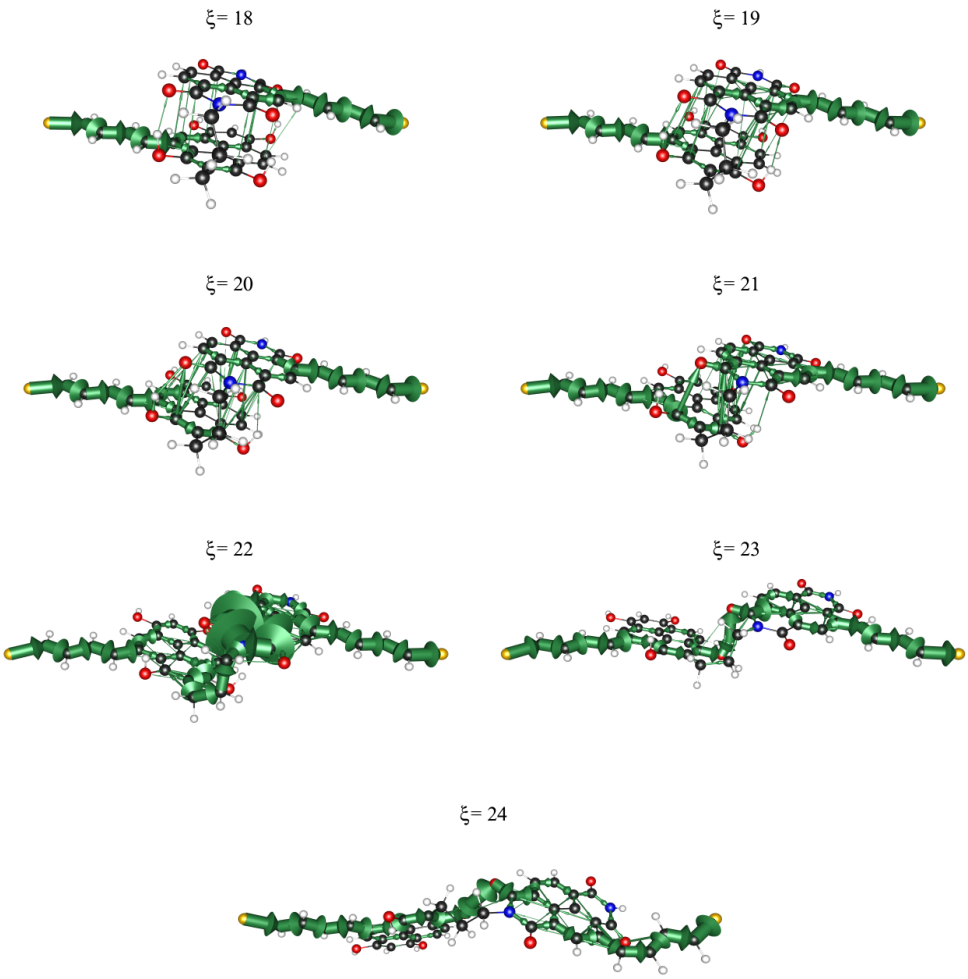

Fig. S 1: **Average local transmission as a function of molecular elongation**. The plots depict the local transmission averaged over 4000 geometries for several values of ξ (in Angstroms). Arrows (solid green) represent the local transmission elements (see Methods for the definition). The radius of each arrow is determined by the magnitude of the transmission element it represents. Plots are normalized so that the S-C components (which are generally very close to the total transmission) are the same in every plot. The total average transmission in each case is shown in Fig. 3 of the paper. Going from $\xi = 18$ Å to $\xi = 24$ Å , the local transmission plots show a change in the dominant conduits for transport through the central region of the system. At shorter extensions ($\xi = 18 - 20$ Å), the transport is dominated by π-stacked interactions with additional small terms between adjacent hydrogen bonds. At longer extensions ($\xi = 23 - 24$ Å), the π-stacked contributions have disappeared, and transport is dominated by coupling through a newly formed hydrogen bond. The plots support the conclusions drawn from Fig. 4 of the paper.

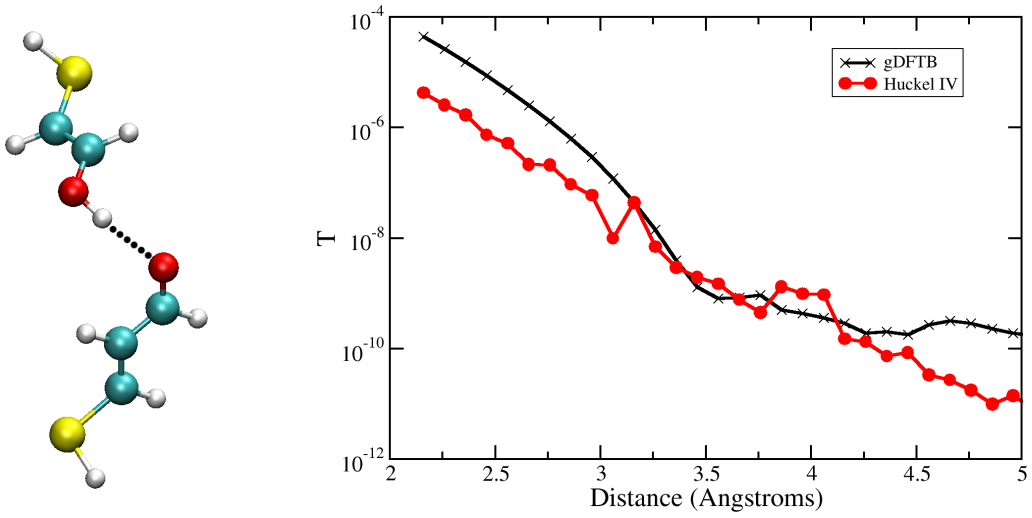

Fig. S 2: **Comparison of the Huckel and gDFTB description of the transmission through hydrogen bonds.** The plot shows the Huckel-IV and gDFTB transmission T as a function of the distance between hydrogen-bonded hydroxy and carbonyl groups in the two molecules in the left panel (HSCHCHOH and HSCHCHCH=O). The molecules are separated along the vector defined by the hydrogen bond (dotted line). Note that for hydrogen-bonding distances below 3 Å, transmission values computed using gDFTB are systematically an order of magnitude greater than those calculated using Huckel-IV. This behavior is manifest in Fig. 3 of the paper. The very limited local basis in the extended Huckel model is largely responsible for this disparity.

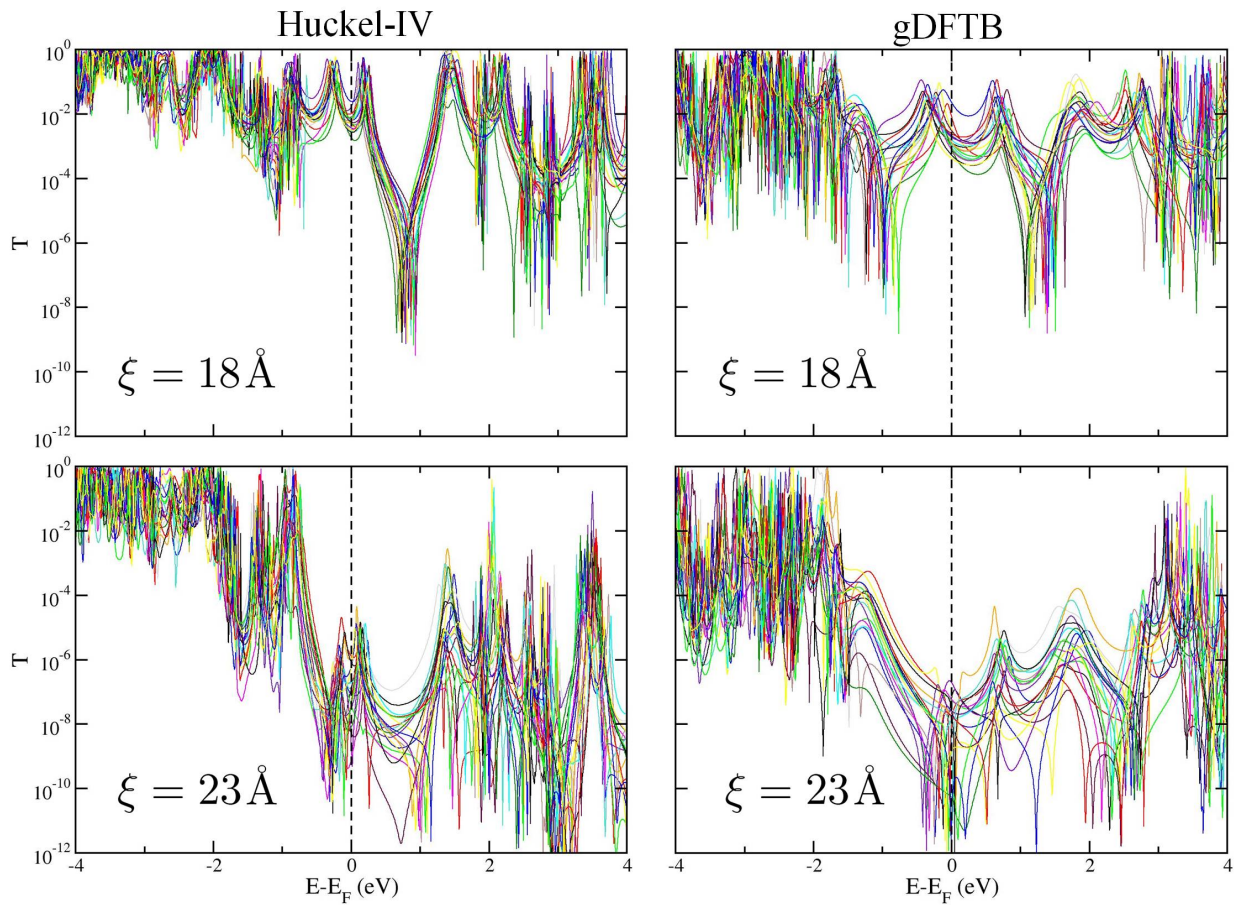

Fig. S 3: **Huckel-IV and gDFTB transmission spectra for selected molecular conformations.** The plots show the transmission $T(E)$ as a function of energy (shifted by the Fermi energy E_F) when the molecular end-to-end distance is fixed at $\xi = 18$ Å (top panels) and $\xi = 23$ Å (bottom panels). In each case, $T(E)$ is plotted for 20 thermally sampled conformations. Different lines correspond to different molecular conformations and the same set of geometries was used in the Huckel-IV and the gDFTB computations. In average, the transmission at the Fermi energy computed by the two methods essentially coincides (recall Fig. 3) even when the transmission for individual conformations can differ substantially. This agreement seems to arise from several confluent factors: (i) the qualitative features of $T(E)$ around the Fermi energy coincide for the two methods; (ii) considerable thermal fluctuations in the transmission curves diminish the importance of the exact location of the Fermi energy and; (iii) the Fermi energy is not near an antiresonance that could lead to dramatic systematic differences between the two methods.